doi:10.3166/acsm.40.25-32 © Lavoisier, Paris

Ann. Chim. Sci. Mat., 2016, 40 (1-2), pp. 25-32

EFFECT OF THE COOLING RATE ON THE ELECTROCHEMICAL BEHAVIOUR OF 2017 ALUMINIUM ALLOY

Zbigniew SZKLARZ[a], Halina KRAWIEC[a], Łukasz ROGAL[b]

a AGH University of Science and Technology, Faculty of Foundry Engineering, 23 Reymonta St., 30-059 Krakow, Poland.
b Institute of Metallurgy and Materials Science of the Polish Academy of Sciences, 25 Reymonta St., 30-059 Krakow, Poland.

Abstract - The influence of cooling rate on the microstructure and on the electrochemical behaviour of 2017 aluminium alloy is studied in this work. The electrochemical measurements were conducted at the mesoscale by using Electrochemical Microcell Technique (EMT) with 300 µm capillary in 0.1 M NaCl aqueous solution. The microstructure of specimens from the internal part of ingot and quick cooled sample were determined by optical microscope and SEM/EDX analysis. The corrosion behavior and the passive properties were studied by means of Open Circuit Potential (OCP) and Electrochemical Impedance Spectroscopy (EIS). It is observed that slow solidification causes irregular grain growth with very large and very small grains. Moreover heterogeneities in the matrix were observed in the form of needle shaped particles. High rate of cooling causes the presence of quite small regular grains and homogenous matrix. The specimens of quick cooled 2017 alloy exhibit higher corrosion potential and the dissolution of metal starts at higher anodic potential compared to the non-treated specimens.

Résumé – Effet de la vitesse de refroidissement sur le comportement électrochimique de l'alliage d'aluminium 2017. L'influence de la vitesse de refroidissement sur la microstructure et sur le comportement électrochimique de l'alliage d'aluminium 2017 a été étudiée dans ce travail. Les mesures électrochimiques ont été réalisées à l'échelle mésoscopique par Technique Electrochimique en Microcellule (EMT) avec un capillaire de 300 µm dans 0,1M NaCl. La microstructure des échantillons de la partie intérieure du lingot et celui obtenu par refroidissement rapide a été caractérisée par microscopie optique et par analyse MEB/EDX. La corrosion et les propriétés de passivation ont été caractérisées par Potentiel de Circuit Ouvert (OCP) et par la Spectroscopie de l'Impédance Electrochimique (EIS). Il est établi qu'une solidification lente provoque une croissance irrégulière des grains de taille très variable dont certains ont la forme d'aguille. Une grande vitesse de refroidissement donne des petits cristallites de forme régulière et une matrice homogène. Les échantillons de l'alliage 2017 refroidis rapidement montrent un potentiel de corrosion plus élevé ainsi que leur potentiel anodique par rapport à des échantillons non-traités.

Tirés-à-part : Z. SZKLARZ, AGH University of Science and Technology, 30-059 Krakow, POLAND

1. INTRODUCTION

It is well known that aluminium alloys have very good mechanical properties (especially after heat treatment called precipitation hardening). Precipitation hardening may be carried out only for alloys where a variable range of the alloy component solubility with temperature occurs. This kind of process conducted on aluminium-copper alloys significantly enhances their tensile strength and hardness [1-5].

The requirements for construction elements are high, thus the corrosion behaviour is also an important factor. Many problems of corrosion processes in AlCu alloys are still unsolved, especially local corrosion processes like pitting corrosion. Small amounts of magnesium and manganese may improve corrosion behavior, as it was shown in the case of 2017 alloy. Susceptibility to local corrosion attack is due to the heterogeneous microstructure containing intermetallic phases and precipitates which are usually present at grain boundaries. It has been shown in several studies that the differences in the chemical composition of the matrix and precipitates are the cause of the differences in the electrochemical potential in high conductivity environments. The authors revealed that some particles which are nobler than the matrix may act as cathodes, whereas particles which are less noble act as anodes [6-11]. In aluminium alloys the cathodic character of intermetallic phases is usually observed. This is the reason of the anodic dissolution of the adjacent matrix [12, 13]. Strongly dissolved matrix, especially at grain boundaries (in these sites precipitates are usually present) is the reason of decreasing mechanical properties.

The process of casting or heat treatment of alloys conducted properly allows for partial dissolution and/or uniform distribution of precipitates. This contributes to improve mechanical properties of the material (hardness, tensile strength) as well as the resistance to corrosion. In 70's Muller et. al. [14, 15] carried out measurements on pure AlCu and AlMg alloys, and they revealed that for supersaturated alloy pitting potential in chlorides is higher than even for pure Al. This indicates that quick cooled 2017 alloy, where copper and magnesium are present (they have variable range of the solubility in aluminium), may have better resistance to corrosion in chlorides. Over time, because of precipitation process, breakdown potential decreases.

In this paper, the results obtained on slow cooled sample (marked **IN**) and quick cooled sample (marked **QC**) of the 2017 alloy are presented.

2. EXPERIMENTAL PROCEDURE

2.1 Specimen preparation

Experiments were performed on aluminium – copper - magnesium alloy marked 2017 (AlCu4Mg1) which is widely used to build heavily loaded components in machine, automotive, aerospace industries. Chemical composition of this alloy (wt. %): 4.5%Cu, 0.6%Mg, 0.8%Mn, 0.4%Si, 0.2%Fe.

Two types of samples were prepared from this alloy: (1) sample cut from **inner** part of the ingot (**IN**), and (2) **quick cooled** sample (**QC**) obtained by sucking melted alloy to cold copper mold.

In *figure 1a* the schematic drawing of the ingot is posted with an indication of the place where sample was cut. Please note that the piece of ingot which is shown in figure 1a comes from big cast (250 mm in diameter and about 8 m long). To study how high cooling rates affect the microstructure and further on the electrochemical behavior, the vacuum suction casting process was employed (*figure 1b*). This method allows obtaining massive samples with very high cooling rates.

In this case, sample from the ingot was remelted by using induction coil and sucked into the cold copper mold by using vacuum pump. In this manner massive quick cooled sample (called QC) with 3 x 2 x 0.2 cm was prepared.
Both IN and QC samples (with a surface area of about 0.5 cm^2) were mechanically polished using diamond pastes and smoothed with a colloidal silica suspension. Samples were cleaned in ethanol and dried in air.

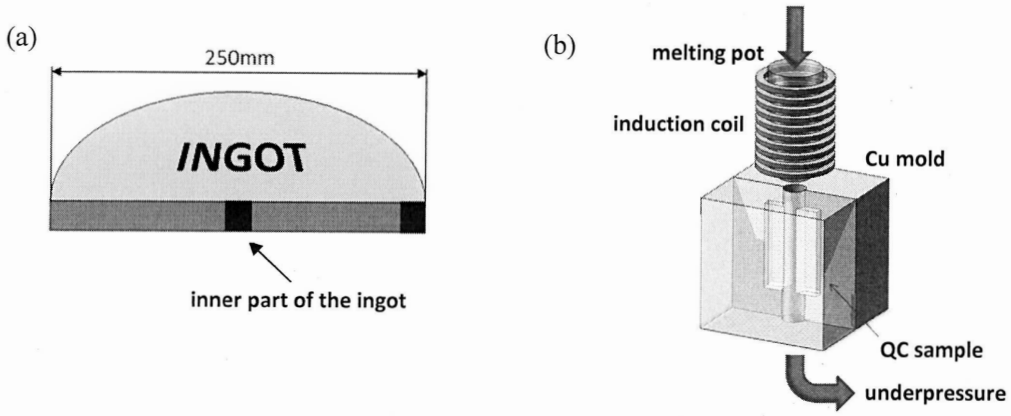

Figure 1. Schematic drawings show: (a) – a peace of ingot and the place where sample IN was cut, (b) – vacuum suction casting process which was used to obtain quick cooled sample (QC).

2.2 Electrochemical measurements at the meso- and microscale

The electrochemical behavior of specimens was studied in 0.1M NaCl solution at room temperature using the electrochemical microcell technique (EMT) which allows measuring the electrochemical behavior at the macro, meso or microscale. This technique consists of a glass micro-capillary that is filled with electrolyte (*figure 2*). The micro-capillary tip was sealed to the specimen surface with a layer of silicon rubber. The microcell (connected with capillary) was mounted on a microscope for precise positioning of the micro-capillary on the surface. The diameter of the capillary tip was in the range of 300 μm for mesoscale. The counter electrode was a platinum wire, and the reference electrode was Ag/AgCl.

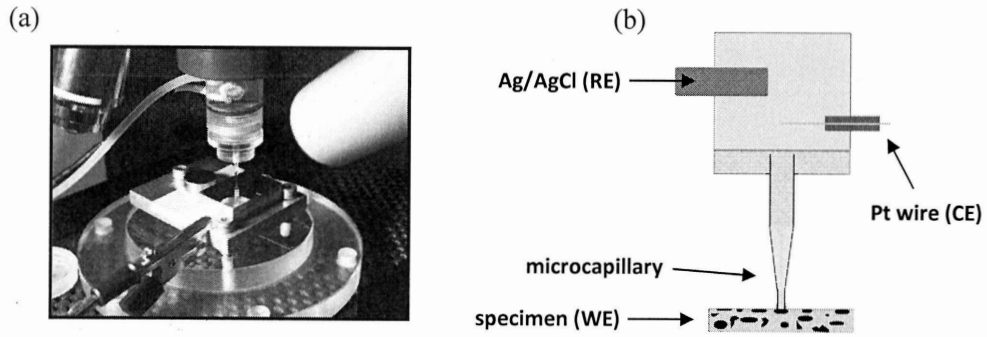

Figure 2. Electrochemical Microcell Technique (EMT) employed in Department of Chemistry and Corrosion of Metals in Krakow: (a) – photo of the system, (b) – the idea of conducting measurements by using EMT.

Using 300 μm capillary it was possible to conduct multiple measurements on one sample, limiting the amount of sample preparation processes (polishing, smoothing). Moreover meso/macro scale measurements using EMT has considerable advantage when samples are small or very thin. The electrochemical behavior was characterized by corrosion potential measurements and electrochemical impedance spectroscopy measurements (EIS). Measurements were carried out on both IN and QC samples in two "tempers": 1/just after mechanical polishing and 2/after 24h ageing in air. Such methodology shows the effect of an air ageing on passive layer properties of both samples.

3. RESULTS AND DISCUSSION

3.1 Microstructure and mechanical properties

Figure 3 shows optical images of the surface of samples: (a) ingot (100x magnification) and (b) QC sample (500x magnification) after mechanical polishing and etching in 2% HF water solution. It is clearly seen that the microstructure of the ingot is heterogeneous and coarse with intermetallic phases at the grain boundaries. Grains have different size (from less than 10 μm in diameter to more than 100 μm). Finer structure is observed in QC sample where grains are less than 10 μm in diameter.

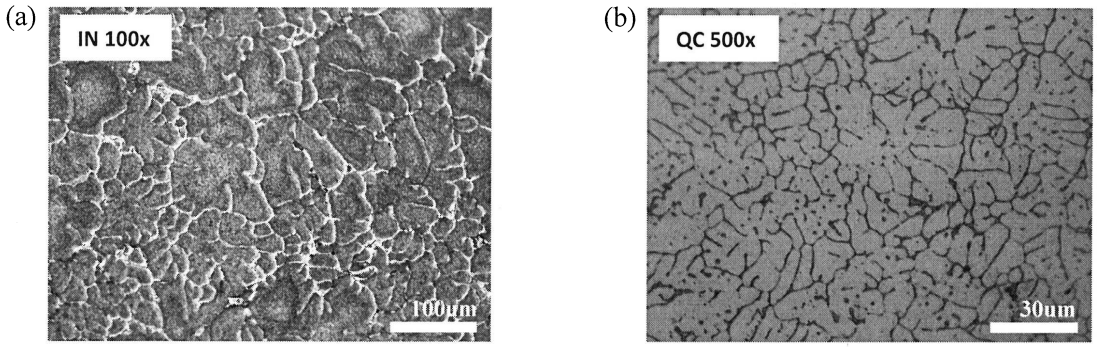

Figure 3. Optical images of the surface of (a) – IN, (b) – QC samples after etching in 2% HF acid water solution.

Figure 4 shows high-resolution images of the microstructure of both samples. The ingot microstructure (*figure 4a*) is composed of two types of large precipitates located at grain boundaries. It was possible to distinguish these two types of precipitates considering the color contrast between each phase in images. The phase appearing in light grey was identified as Al_2Cu and those appearing in dark colors as a mixture of Al-Si-Mn-Fe-Cu. Moreover, high-resolution images reveal the presence of heterogeneities in the matrix of the alloy. It is clearly seen that needle shaped particles enriched in copper are located inside grains [12].

SEM image of QC sample after mechanical polishing is shown in *figure 4b*. As it was already mentioned, the microstructure contains small grains and fine eutectic located at grain boundaries. The statistical analysis of the chemical composition conducted at grain boundaries reveals that they are composed of Al-Cu-Mn-Fe-Si-Mg. However, additional studies are needed to confirm the chemical composition of this phase. The chemical composition of the matrix indicates that the solid solution is supersaturated with about 0.5at.% of Cu. Please note that no small particles were

observed by using LM and SEM techniques. Chemical elements distribution is more homogeneous than in previous case both in precipitates and in the matrix.

After vacuum suction casting process, the mechanical properties changed in favor of QC sample. The hardness of QC sample increases (95 HV_5). This increase is related with the finer structure and the supersaturated solid solution. The hardness of the ingot was 85 HV_5.

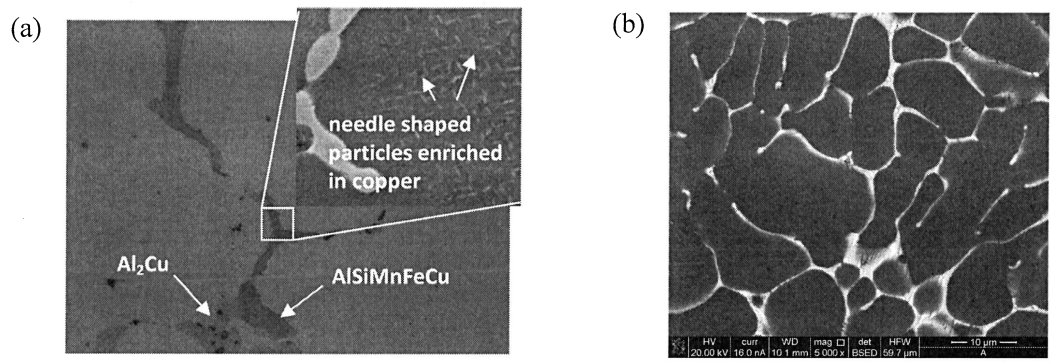

Figure 4. (a) – optical and SEM (in the corner) images showing the microstructure of IN sample after mechanical polishing where Al_2Cu phase (light), AlSiMnFeCu phase (dark) and heterogeneities in matrix are visible; (b) – SEM image of QC sample after mechanical polishing.

3.2 Electrochemical measurements

In order to study the electrochemical behaviour of both specimens (IN and QC), linear sweep voltamperometry curves have been plotted (*figure 5*). For the ingot (IN) and the quick cooled (QC) specimens, a sharp increase of the anodic current density is observed in the anodic domain as soon as the corrosion potential is reached (no passive range). The polarization curve of the QC specimen exhibits a large cathodic domain, leading to a shift of the corrosion potential to the anodic direction. This behavior suggests that the 2017 aluminium alloy after quick cooling has better corrosion resistance than the ingot.

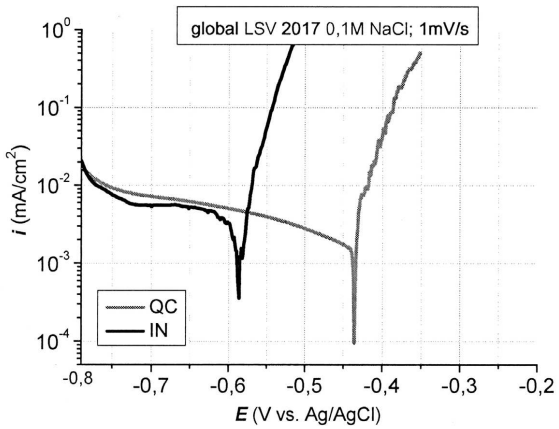

Figure 5. Global polarization curves plotted for IN and QC specimens in 0.1 M NaCl solution. Potential scan rate 1 mV/s.

In order to compare the passive properties and corrosion resistance of the ingot and the quick cooled aluminium alloy, the open circuit potential and EIS measurements at mesoscale have been performed (*figures 6 and 7*). Electrochemical Impedance Spectroscopy measurements were carried out by using 300 μm capillary filled with 0.1M NaCl water solution. Impedance measurements were plotted at the corrosion potential with a 10 mV potential perturbation.

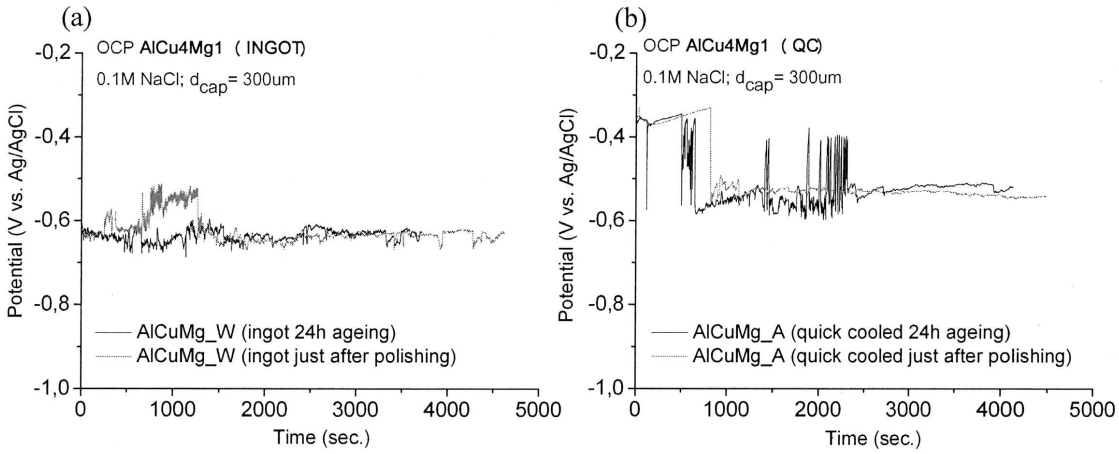

Figure 6. Evolution of the open circuit potential for: (a) - IN and (b) - QC specimens in 0.1 M NaCl solution after polishing (grey curves) and after ageing for 24 hours (black curves).

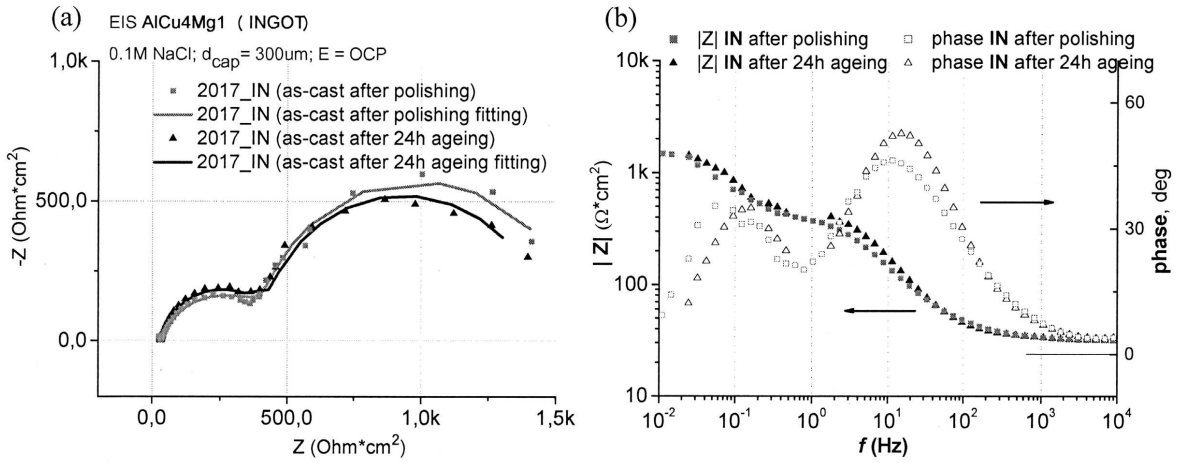

Figure 7. (a) Nyquist and (b) Bode plots obtained for the IN sample before (grey squares) and after 24 hours air ageing (black triangles).

Measurements have been performed after mechanical polishing and after 24-hour ageing in air. No significant differences were observed between curves obtained after polishing and after 24-hour ageing in air. By contrast, significant difference in the OCP is observed between the IN and QC specimens. The corrosion potential of the QC specimen (of about -530 mV vs. Ag/AgCl), was nobler than that of the ingot (values around -630 mV vs. Ag/AgCl). Such difference suggests that the quick cooled aluminium alloy has higher resistance to corrosion than the ingot. This results confirm the results obtained from the polarization curves (*figure 5*).

Figures 7 and 8 show the EIS diagrams obtained for the ingot (IN) and the quick cooled (QC) samples, respectively. It is clearly seen that diagrams of both samples are composed of two capacitive loops. At the OCP value, both anodic and cathodic reactions occur. To determine which loop is connected with cathodic processes, additional EIS diagrams have to be plotted under potentiostatic control (with applied potential in the cathodic domain). Previous results on duplex stainless steels [16] show that the loop at high frequencies can be assigned to the charge transfer for oxygen reduction. The second loop at low frequencies can then be connected with the passive film, and eventually the formation of corrosion products.

Impedance spectra have been fitted using the equivalent circuit visible in *figure 9*, where: *R1* is the electrolyte resistance; *R2* the charge transfer resistance associated with the oxygen reduction, *CPE1* the constant phase element associated with the double layer, *R3* the polarization resistance associated with the passive film and corrosion products, *CPE2* the constant phase element of the surface films. Numerical data derived from the fitting procedure are reported in *table I*.

Ageing in air for 24 hours has nearly no influence of the electrochemical behavior of the IN sample (*table I*). By contrast, ageing has significant influence on the behavior of the QC sample. The resistances and CPE values are increased, indicating that the sample has better corrosion resistance after ageing. Such behaviour is determined by the microstructure obtained after quick cooling process. In addition, the resistance values found for the QC specimen are also higher than for the IN sample, indicating that it has better corrosion resistance. A more homogeneous distribution of the alloying elements in the matrix, the presence of small grains and fine eutectic located at the grain boundaries improve the passive properties and the corrosion resistance of the aluminium alloy.

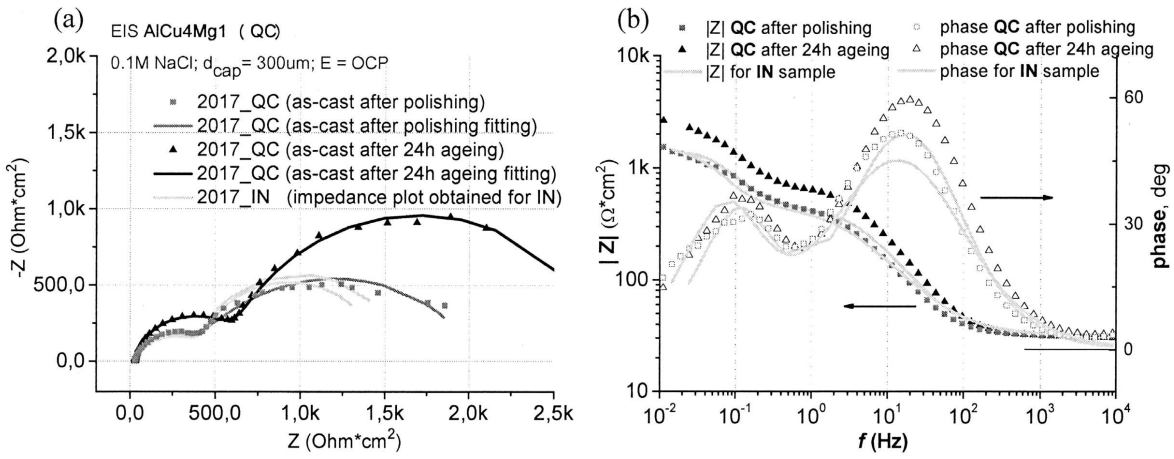

Figure 8. (a) Nyquist and (b) Bode plots obtained on the QC sample after polishing (grey squares) and after 24-hour ageing in air (black triangles). For comparison purpose, impedance diagrams of the IN sample are also reported (grey curves).

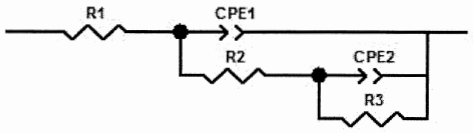

Figure 9. Electrical equivalent circuit used to fit impedance plots of IN and QC samples.

Table I. Numerical data derived from fitting of EIS spectra.

	IN sample						
	R1 ***(Ω*cm^2)***	***CPE1*** ***(Ω^{-1}.cm^{-2} s$^{\varphi}$)***	***CPE1-φ***	***R2*** ***(Ω*cm^2)***	***CPE2*** ***(Ω^{-1}.cm^{-2} s$^{\varphi}$)***	***CPE2-φ***	***R3*** ***(Ω*cm^2)***
polishing	31.8	0.27 10^{-3}	0.778	452.6	3.4 10^{-3}	0.998	1115
ageing	32.5	0.15 10^{-3}	0.876	441.5	2.5 10^{-3}	0.998	992
	QC sample						
polishing	31.2	0.17 10^{-3}	0.888	395	2.4 10^{-3}	0.713	1660
ageing	31	0.09 10^{-3}	0.913	658	1.5 10^{-3}	0.905	2126

4. CONCLUSIONS

- vacuum suction casting method allows to obtain samples with improved mechanical properties as well as corrosion resistance,
- corrosion resistance is higher what is related with fine microstructure (both eutectic and grains),
- quick cooling process allows to modify the matrix which is supersaturated with copper, this according to the literature improve corrosion resistance (especially pitting – what has been shown on LSV),
- EIS measurements revealed that modification of 2017 alloy also modify the structure of passive layer (however additional studies are needed to analyze structure of such passive layer).

5. REFERENCES

[1] J.G. Kaufman, E.L. Rooy, Aluminium Alloy Castings: Properties, Processes and Applications, 2004.
[2] J.R.Brown: Foseco Non-Ferrous Foundryman's Handbook, 1999.
[3] I. J. Polmear: Light Alloys - From Traditional Alloys to Nanocrystals, 2006.
[4] V. S. Zolotorevsky, N. A. Belov, M. V. Glazoff, Casting Aluminium Alloys, 2007.
[5] L. Katgerman, D. Eskin, Hardening, Annealing, and Aging, Handbook of Aluminium, Vol. 1 Physical Metallurgy and Processes, 2003.
[6] N. Birbilis, R.G. Bucheit, J. Electrochem. Soc., 152 (2005) B140-B151.
[7] K. Nisancioglu, J. Electrochem. Soc., 137 (1990) 69-77.
[8] V. Guillaumin, G. Mankowski, Corr Sci., 41 (1999) 421-498.
[9] P. Campestrini, E.P.M. van Vesting, H.W. van Rooijen, J.H.W. de Wit, Corr Sci., 42 (2000) 1853-1861.
[10] D.A. Little, B.J. Connoly, J.R. Scully, Corr. Sci., 49 (2007) 347-372.
[11] R. Ambat, A.J. Davenport, G.M. Scamans, A. Afseth, Corr Sci., 48 (2006) 3455-3471.
[12] H. Krawiec, V. Vignal, Z. Szklarz, J. Solid St. Electrochem., 13 (2008) 1181-1191.
[13] H. Krawiec, Z. Szklarz, V. Vignal, Corr. Sci., 65 (2012) 387-396.
[14] I. L. Muller, J. L. Galvele, Corr. Sci., 17 (1977) 179-189.
[15] I. L. Muller, J. L. Galvele, Corr Sci., 17 (1977) 995-1007.
[16] V. Vignal, H. Krawiec, O. Heintz, D. Mainy, Corr. Sci., 67 (2013) 109-117.

(Article reçu le 01/10/2015, sous forme définitive le 07/01/2016).